

Thermal lattice Boltzmann equation for low Mach number flows: Decoupling model

Zhaoli Guo,* Chuguang Zheng, and Baochang Shi

National Laboratory of Coal Combustion, Huazhong University of Science and Technology, Wuhan, People's Republic of China

T. S. Zhao

Department of Mechanical Engineering, Hong Kong University of Science and Technology, Kowloon, Hong Kong

(Received 4 November 2006; published 14 March 2007)

A lattice Boltzmann model is proposed for solving low Mach number thermal flows with viscous dissipation and compression work in the double-distribution-function framework. A distribution function representing the total energy is defined based on a single velocity distribution function, and its evolution equation is derived from the continuous Boltzmann equation. A lattice Boltzmann equation model with clear physics and a simple structure is then obtained from a kinetic model for the decoupled hydrodynamic and energy equations. The model is tested by simulating a thermal Poiseuille flow and natural convection in a square cavity, and it is found that the numerical results agree well with the analytical solutions and/or the data reported in previous studies.

DOI: [10.1103/PhysRevE.75.036704](https://doi.org/10.1103/PhysRevE.75.036704)

PACS number(s): 47.11.-j, 44.05.+e

I. INTRODUCTION

Although the lattice Boltzmann equation (LBE) method has achieved great success in simulating athermal and isothermal fluid flows, its applications for thermohydrodynamics is still not satisfactory. Constructing LBE models for thermal flows remains challenging in the LBE community, although some efforts have been made from various viewpoints. A recent comprehensive review on this topic can be found elsewhere [1].

The existing strategies for constructing thermal LBE (TLBE) models can be classified into three categories, i.e., the multispeed approach, the double-distribution-function (DDF) approach, and the hybrid approach. The multispeed approach is a straightforward extension of the athermal LBE, in which only the velocity distribution function (VDF) is used [3–5]; the DDF approach utilizes two different distribution functions (DFs), one for the velocity field and the other for the temperature or internal energy field; the hybrid approach is similar to the DDF approach except that the energy equation is solved by different numerical methods (e.g., finite-difference or finite-volume methods) rather than by solving the LBE [1].

Both the multispeed and DDF approaches have some limitations [2]. The multispeed models usually suffer from severe numerical instability and the temperature variation simulated is limited to a narrow range, and usually results in a fixed Prandtl number, although some later versions have overcome this problem [6]. For DDF LBE models, although they exhibit good numerical stability and an adjustable Prandtl number [7–23], most of them (except for those proposed in Refs. [9,13]) take no account of the viscous dissipation and compression work.

The first DDF model that incorporates viscous dissipation and compression work is attributed to He, Chen, and Doolen (HCD) [9], where an additional DF is defined for the fluid

temperature and is derived directly from the moment of the VDF. This model has attracted much attention since its emergence, and has found applications in a variety of fields [15–23]. Despite the apparent advantages of the HCD TLBE model, it is well recognized that this model still suffers from some deficiencies. For instance, both the LBE for the temperature distribution function (TDF) and the calculation of the temperature include complicated terms involving temporal and spatial derivatives of the macroscopic flow variables, which may introduce some additional errors and do harm to the numerical stability. Furthermore, in the derivation of the equilibrium for the TDF, an *ad hoc* regrouping technique was employed so that some high-order terms could be neglected. The regrouping is somewhat arbitrary, and different regrouping methods may lead to different equilibria [9,13]. It is noted that some improved versions have been proposed by some groups. For instance, a simplified model was derived by dropping the spatial gradient term in the temperature LBE for thermal fluids where viscous heat dissipation and compression work are neglected [12], which is similar to other DDF LBE models that do not consider the viscous and compression effects on the energy. Recently, Shi *et al.* proposed another version by regrouping the Taylor expansions of the continuous equilibrium for the TDF [13]. Unfortunately, the complicated spatial gradient terms still exist in the model if viscous dissipation is included.

In this paper, we aim to propose an alternative TLBE model, in which viscous dissipation and compression work are considered in the DDF framework. To this end, we first introduce a distribution function that represents the total energy rather than the temperature (or internal energy) as the second DF in addition to the VDF. Then we construct a kinetic equation for the total energy distribution function (TEDF) based on the kinetic equation for the VDF. Based on a kinetic model constituted of two kinetic equations (for the VDF and TEDF, respectively), a discrete velocity model (DVM) is proposed by choosing an appropriate discrete velocity set based on a Hermite expansion of the equilibrium for the VDF and TEDF. Further discretizations of the temporal and spatial derivatives of the DVM lead to our TLBE. It

*Corresponding author. Electronic address: zlguo@hust.edu.cn

should be noted that, unlike the HCD model, the use of the TEDF enables the proposed LBE model to be simpler without the complicated spatial gradient terms; and the expansion of the continuous equilibrium for the TEDF into a series of tensor Hermite polynomials instead of Taylor series allows the discrete equilibrium to be determined uniquely.

The rest of the paper is organized as follows. In Sec. II, the DF for the total energy is introduced and its kinetic equation is constructed based on the Boltzmann equation. In Sec. III, a discrete velocity model is developed from the kinetic equations by expanding the energy DF into a series of tensor Hermite polynomials and applying the Gauss-Hermit quadrature to the velocity moments of the DF. Section IV presents the derivation of the thermal LBE model from the DVM by employing some standard numerical procedures. Numerical tests of the LBE model are made in Sec. V by simulating thermal Poiseuille flow and natural convection in a square cavity, and finally a brief summary is given in Sec. VI.

II. KINETIC MODEL WITH DIFFERENT MOMENTUM AND ENERGY RELAXATION TIMES

A. Kinetic models of Bhatnagar-Gross-Krook type

In kinetic theory, a monatomic gas is described by the velocity distribution function $f(\mathbf{x}, \boldsymbol{\xi}, t)$ of the molecules, which is defined such that $f d\boldsymbol{\xi} d\mathbf{x}$ is the probability of finding a molecule moving with velocity $\boldsymbol{\xi}$ at position \mathbf{x} and time t . The evolution of the VDF is governed by the Boltzmann equation [24]

$$\partial_t f + \boldsymbol{\xi} \cdot \nabla f + \mathbf{a} \cdot \nabla_{\boldsymbol{\xi}} f = \Omega_f, \quad (1)$$

where \mathbf{a} is the acceleration, and Ω_f is a collision operator that satisfies the following conservation laws:

$$\int \phi_\alpha \Omega_f d\boldsymbol{\xi} = 0, \quad (2)$$

where $\phi = (1, \boldsymbol{\xi}, |\boldsymbol{\xi}|^2)$. The original Boltzmann collision operator is a complicated integral that depends on the interparticle potentials. In practical applications, Ω_f is usually approximated by some simplified models. One widely used approximation is the so-called single-relaxation-time or Bhatnagar-Gross-Krook (BGK) model [25]

$$\Omega_f = -\frac{1}{\tau_f} [f - f^{(eq)}], \quad (3)$$

where τ_f is the relaxation time, and $f^{(eq)}$ is the local Maxwellian equilibrium distribution function (EDF) defined by

$$f^{(eq)}(\boldsymbol{\xi}; \rho, \mathbf{u}, T) = \frac{\rho}{(2\pi RT)^{D/2}} \exp\left(-\frac{(\boldsymbol{\xi} - \mathbf{u})^2}{2RT}\right), \quad (4)$$

with D being the spatial dimension and R the gas constant. The fluid variables in the EDF, i.e., the density ρ , velocity \mathbf{u} , and temperature T , are defined as the moments of f ,

$$\begin{pmatrix} \rho \\ \rho \mathbf{u} \\ \frac{D\rho RT}{2} \end{pmatrix} = \begin{pmatrix} \int f d\boldsymbol{\xi} \\ \int \boldsymbol{\xi} f d\boldsymbol{\xi} \\ \int \frac{(\boldsymbol{\xi} - \mathbf{u})^2}{2} f d\boldsymbol{\xi} \end{pmatrix}. \quad (5)$$

Although the BGK model retains the main features of the original Boltzmann collision operator, it is limited to gases with a fixed Prandtl number [24], which has been recognized as one of the main defects of the model. Some efforts have been made to overcome the fixed Prandtl number problem of the BGK model. For instance, one can use the so-called ellipsoidal statistical BGK (ESBGK) model where the Maxwell EDF is replaced with an anisotropic Gaussian EDF [26], or use a velocity-dependent relaxation time [27]. Alternatively, Wood directly introduced two relaxation times into the nonequilibrium distribution function after noticing that the momentum and energy should have different transport time scales during the collision process [28].

Recently, He *et al.* proposed another approach to fix the Prandtl number problem by introducing a new variable (the so-called internal energy distribution function) as an (internal) energy DF,

$$g = \frac{(\boldsymbol{\xi} - \mathbf{u})^2}{2} f. \quad (6)$$

A BGK-type kinetic equation for g is then constructed based on the Boltzmann equation (1), which allows for the energy having a relaxation time scale different from that of the momentum transport:

$$\partial_t g + \boldsymbol{\xi} \cdot \nabla g = -\frac{1}{\tau_g} [g - g^{(eq)}] - fq, \quad (7)$$

where τ_g is the relaxation time for the energy transport, and $g^{(eq)}$ is the corresponding energy EDF defined by

$$g^{(eq)} = \frac{\rho(\boldsymbol{\xi} - \mathbf{u})^2}{2(2\pi RT)^{D/2}} \exp\left(-\frac{(\boldsymbol{\xi} - \mathbf{u})^2}{2RT}\right). \quad (8)$$

The quantity q in Eq. (7) is given by

$$q = (\boldsymbol{\xi} - \mathbf{u}) \cdot [\partial_t \mathbf{u} + \boldsymbol{\xi} \cdot \nabla \mathbf{u}]. \quad (9)$$

In this model, the density and velocity are still determined by the moments of the density DF f as Eq. (5), but the internal energy $\epsilon \equiv DRT/2$ is now defined by the energy DF g :

$$\rho \epsilon = \int g d\boldsymbol{\xi}. \quad (10)$$

Through a Chapman-Enskog analysis, He *et al.* were able to show that the macroscopic equations derived from Eqs. (1) and (7) could have a proper Prandtl number given that τ_g is chosen appropriately [9].

In essence, the approach used by the HCD model is identical to that proposed by Woods where two relaxation times are used to distinguish the momentum and energy transport due to particle collisions. The main difference between these

two approaches lies in the realization of the time scale separation: In the method of Woods, the two relaxation times are directly applied to the first-order approximation of the VDF f in the Chapman-Enskog expansion, while the HCD model separates the energy transport from the momentum transport with two time scales explicitly. It is difficult to construct a LBE model based on Woods' method directly since the Chapman-Enskog expansion cannot be employed in the LBE explicitly. On the contrary, the HCD model can serve as a good base for the LBE [9]. However, the term fq in the kinetic equation for the energy DF of the HCD model makes the final LBE model contain some terms involving spatial gradients of both the density and velocity. These terms not only make the LBE model more computationally expensive and may do harm to the numerical stability, but also may lead to some unphysical phenomena in fluid systems containing large spatial gradients, such as multiphase or multicomponent and microscale flows.

B. Total energy distribution function and its kinetic equation

Unlike the HCD model, which uses the internal energy distribution function g , here we introduce the following *total energy* distribution function:

$$h = \frac{\xi^2}{2} f, \quad (11)$$

from which the total energy E can be defined as

$$\rho E = \rho \left(\epsilon + \frac{\mathbf{u}^2}{2} \right) = \int h d\xi. \quad (12)$$

The evolution of h can be obtained from the Boltzmann equation (1) as

$$\partial_t h + \xi \cdot \nabla h + \mathbf{a} \cdot (\nabla_\xi h - \xi f) = \Omega_h, \quad (13)$$

where $\Omega_h = \xi^2 \Omega_f / 2$ is the collision operator characterizing the energy change during the particle collisions.

The key point for developing a kinetic model based on the total energy DF h is to specify the collision term Ω_h in Eq. (13) with sound physics. By noting that the contribution of Ω_h includes the internal energy part and the mechanical energy part, we first decompose Ω_h into these two parts:

$$\Omega_h = \Omega_i + \Omega_m, \quad (14)$$

where $\Omega_i = (\xi - \mathbf{u})^2 \Omega_f / 2$ is the internal energy part, and

$$\Omega_m = \Omega_h - \Omega_i = \left(\frac{\xi^2}{2} - \frac{(\xi - \mathbf{u})^2}{2} \right) \Omega_f \equiv Z \Omega_f$$

is the mechanical energy part, with $Z = \xi \cdot \mathbf{u} - \mathbf{u}^2 / 2$. According to Woods' theory [28], Ω_m should have the same time scale as that of Ω_f , and therefore we approximate it as

$$\Omega_m = -\frac{Z}{\tau_f} (f - f^{(eq)}). \quad (15)$$

For the internal energy part, we can approximate it with another BGK-type model as in the HCD model, i.e., $\Omega_i = -\tau_g^{-1} (g - g^{(eq)})$. But such a model will introduce the internal

energy DF g as an auxiliary variable. In order to avoid this inconvenience, we replace g with $h - Zf$, and thus obtain the following BGK-type model:

$$\Omega_i = -\frac{1}{\tau_h} [(h - h^{(eq)}) - Z(f - f^{(eq)})], \quad (16)$$

where $\tau_h = \tau_g$ is the relaxation time characterizing the internal energy change during the particle collisions, and $h^{(eq)} \equiv \xi^2 f^{(eq)} / 2$ is the corresponding EDF. As such, the final collision operator Ω_h is given by

$$\Omega_h = -\frac{1}{\tau_h} (h - h^{(eq)}) + \frac{Z}{\tau_{hf}} (f - f^{(eq)}), \quad (17)$$

where

$$\frac{1}{\tau_{hf}} = \frac{1}{\tau_h} - \frac{1}{\tau_f}.$$

It is clear that, as $\tau_h = \tau_f$, the second term of Ω_h vanishes and the model is identical to the original BGK model. Otherwise, the second term can be viewed as a correction to the single-relaxation-time model. As will be seen later, without this term, the model gives incorrect viscous heat dissipation in the energy equation, although the Prandtl number can be tuned to be correct.

In summary, we propose the following two-relaxation-time model for describing a thermal fluid system with a variable Prandtl number:

$$\partial_t f + \xi \cdot \nabla f + \mathbf{a} \cdot \nabla_\xi f = -\frac{1}{\tau_f} (f - f^{(eq)}), \quad (18a)$$

$$\partial_t h + \xi \cdot \nabla h + \mathbf{a} \cdot \nabla_\xi h = -\frac{1}{\tau_h} (h - h^{(eq)}) + \frac{Z}{\tau_{hf}} (f - f^{(eq)}) + f \xi \cdot \mathbf{a}, \quad (18b)$$

where

$$f^{(eq)} = \frac{\rho}{(2\pi RT)^{D/2}} \exp\left(-\frac{(\xi - \mathbf{u})^2}{2RT}\right), \quad (19a)$$

$$h^{(eq)} = \frac{\rho \xi^2}{2(2\pi RT)^{D/2}} \exp\left(-\frac{(\xi - \mathbf{u})^2}{2RT}\right). \quad (19b)$$

The fluid variables are defined as

$$\begin{pmatrix} \rho \\ \rho \mathbf{u} \\ \rho E \end{pmatrix} = \begin{pmatrix} \int f d\xi \\ \int \xi f d\xi \\ \int h d\xi \end{pmatrix}. \quad (20)$$

Through the Chapman-Enskog expansion, we can obtain the following hydrodynamic equations at the Navier-Stokes level (see Appendix A for details):

$$\partial_t \rho + \nabla \cdot (\rho \mathbf{u}) = 0, \quad (21a)$$

$$\partial_t(\rho\mathbf{u}) + \nabla \cdot (\rho\mathbf{u}\mathbf{u}) = -\nabla p + \nabla \cdot \boldsymbol{\tau} + \rho\mathbf{a}, \quad (21b)$$

$$\partial_t(\rho E) + \nabla \cdot [(p + \rho E)\mathbf{u}] = \nabla \cdot (\lambda \nabla T) + \nabla \cdot (\boldsymbol{\tau} \cdot \mathbf{u}) + \rho\mathbf{u} \cdot \mathbf{a}, \quad (21c)$$

where $p = \rho RT$ is the pressure, $\boldsymbol{\tau} = \mu[\mathbf{S} - (2/D)(\nabla \cdot \mathbf{u})\mathbf{I}]$ ($S_{\alpha\beta} = \partial_\alpha u_\beta + \partial_\beta u_\alpha$) is the viscous stress tensor, and the viscosity and thermal conductivity are given by

$$\mu = \tau_f p \quad \text{and} \quad \lambda = \frac{(D+2)R}{2} \tau_h p = c_p \tau_h p,$$

respectively, where $c_p = (D+2)R/2$ is the specific heat coefficient at constant pressure. Using the momentum equation (21b), we can deduce the temperature equation from the total energy equation (21c) as

$$c_v[\partial_t(\rho T) + \nabla \cdot (\rho\mathbf{u}T)] = \nabla \cdot (\lambda \nabla T) - p \nabla \cdot \mathbf{u} + \boldsymbol{\tau} \cdot \nabla \mathbf{u}, \quad (22)$$

where $c_v = DR/2$ is the specific heat coefficient at constant volume. The Prandtl number of the system, $\text{Pr} = \mu c_p / \lambda = \tau_f / \tau_h$, can be made arbitrary by tuning the two relaxation times. This result is just the same as that of the Woods' model [28].

We would like to point out that the above kinetic model can also be extended to polyatomic gases. In such a case, the VDF f is also a function of the rotational and/or vibrational energies that can be either discrete or continuous [27]. In the continuous case, f can be expressed as $f = f(x, \boldsymbol{\xi}, \boldsymbol{\eta}, t)$, where $\boldsymbol{\eta}$ is a vector containing K components corresponding to the internal freedoms. Accordingly, a BGK-type model can be used to approximate the collision operator [29]:

$$\partial_t f + \boldsymbol{\xi} \cdot \nabla f + \mathbf{a} \cdot \nabla_{\boldsymbol{\xi}} f = \frac{1}{\tau_f} (f - f^{(eq)}), \quad (23)$$

where

$$f^{(eq)} = \frac{\rho}{(2\pi RT)^{(D+K)/2}} \exp\left(-\frac{(\boldsymbol{\xi} - \mathbf{u})^2 + \boldsymbol{\eta}^2}{2RT}\right), \quad (24)$$

and the fluid variables are now defined as

$$\begin{pmatrix} \rho \\ \rho\mathbf{u} \\ \frac{(D+K)\rho RT}{2} \end{pmatrix} = \begin{pmatrix} \int f d\boldsymbol{\xi} d\boldsymbol{\eta} \\ \int \boldsymbol{\xi} f d\boldsymbol{\xi} d\boldsymbol{\eta} \\ \int \frac{(\boldsymbol{\xi} - \mathbf{u})^2 + \boldsymbol{\eta}^2}{2} f d\boldsymbol{\xi} d\boldsymbol{\eta} \end{pmatrix}. \quad (25)$$

By introducing two reduced DFs, $\bar{f} = \int f d\boldsymbol{\eta}$ and $\bar{h} = \int (\boldsymbol{\xi}^2 + \boldsymbol{\eta}^2)/2 f d\boldsymbol{\eta}$, we can obtain the following two kinetic equations from the Boltzmann equation (1):

$$\partial_t \bar{f} + \boldsymbol{\xi} \cdot \nabla \bar{f} + \mathbf{a} \cdot \nabla_{\boldsymbol{\xi}} \bar{f} = -\frac{1}{\tau_f} (\bar{f} - \bar{f}^{(eq)}), \quad (26a)$$

$$\partial_t \bar{h} + \boldsymbol{\xi} \cdot \nabla \bar{h} + \mathbf{a} \cdot \nabla_{\boldsymbol{\xi}} \bar{h} = -\frac{1}{\tau_h} (\bar{h} - \bar{h}^{(eq)}) + \frac{Z}{\tau_{hf}} (\bar{f} - \bar{f}^{(eq)}) + \bar{f} \boldsymbol{\xi} \cdot \mathbf{a}, \quad (26b)$$

where

$$\bar{f}^{(eq)} = \int f^{(eq)} d\boldsymbol{\eta} = \frac{\rho}{(2\pi RT)^{D/2}} \exp\left(-\frac{(\boldsymbol{\xi} - \mathbf{u})^2}{2RT}\right), \quad (27a)$$

$$\bar{h}^{(eq)} = \int \frac{\boldsymbol{\xi}^2 + \boldsymbol{\eta}^2}{2} f^{(eq)} d\boldsymbol{\eta} = \frac{\rho(\boldsymbol{\xi}^2 + KRT)}{2(2\pi RT)^{D/2}} \exp\left(-\frac{(\boldsymbol{\xi} - \mathbf{u})^2}{2RT}\right). \quad (27b)$$

The fluid variables are defined now as

$$\begin{pmatrix} \rho \\ \rho\mathbf{u} \\ \rho E \end{pmatrix} = \begin{pmatrix} \int \bar{f} d\boldsymbol{\xi} \\ \int \boldsymbol{\xi} \bar{f} d\boldsymbol{\xi} \\ \int \bar{h} d\boldsymbol{\xi} \end{pmatrix}. \quad (28)$$

The macroscopic equations derived from the model are the same as those given in Eq. (21), but in the energy equation the specific heats c_v and c_p include now the contribution of the rotational and/or vibrational energies, i.e., $c_v = (D+K)R/2$ and $c_p = (D+K+2)R/2$.

III. THE DISCRETE VELOCITY MODEL

Previous studies have shown that we can derive a LBE model from a given kinetic model following some standard procedures [30–32]. In such an approach, a discrete velocity model is first constructed by discretizing the velocity space of the continuous kinetic equation into a finite set of discrete velocities, and then the LBE model is obtained by discretizing the temporal and spatial derivations of the DVM, using some standard numerical schemes. The key point for developing LBE models following this approach lies in the first step, i.e., the derivation of the discrete velocity set so that the DVM can match the original kinetic model with sufficient accuracy. In this section, we will concentrate on this step and present a DVM for thermal flows based on the kinetic model proposed in Sec. II.

A. Hermite expansions of the equilibrium distribution functions

In order to obtain the correct hydrodynamic equations, the velocity space of the kinetic model must be discretized with sufficient accuracy, or, in other words, the physical symmetry of the resulting discrete velocity set should be adequate. To this end, it has been suggested to expand the EDF $f^{(eq)}$ around the state at rest under the condition of low Mach number, either by performing a Taylor series expansion up to \mathbf{u}^2 [9,30,31], or by projecting $f^{(eq)}$ onto the tensor Hermite polynomial basis in terms of the particle velocity $\boldsymbol{\xi}$ and up to the second order [32]. For isothermal flows, both expansions

give the same results. For thermal flows, however, the two methods will result in different formulations. In the present work, we prefer to use the projection method because the expansion coefficients obtained in this way are just the velocity moments of the distribution function, and the truncation of higher-order terms do not directly alter the lower-order moments of the distribution function.

The Hermite expansions of $f^{(eq)}$ and $h^{(eq)}$ given by Eqs. (27a) and (27b) can be expressed as

$$f^{(eq)} = \omega(\xi, T) \sum_n \frac{A_\alpha^{(n)}(\mathbf{x}, t)}{n!} H_\alpha^{(n)}(\hat{\xi}), \quad (29a)$$

$$h^{(eq)} = \omega(\xi, T) \sum_n \frac{B_\alpha^{(n)}(\mathbf{x}, t)}{n!} H_\alpha^{(n)}(\hat{\xi}), \quad (29b)$$

where

$$\omega(\xi, T) = \frac{1}{(2\pi RT)^{D/2}} \exp\left(-\frac{\xi^2}{2RT}\right),$$

and $\hat{\xi} = \xi/\sqrt{RT}$; $H_\alpha^{(n)}$ are the n th-order tensor Hermite polynomials. The expansion coefficients in Eq. (29), $A_\alpha^{(n)}$ and $B_\alpha^{(n)}$, are given by

$$A_\alpha^{(n)} = \int f^{(eq)} H_\alpha^{(n)}(\hat{\xi}) d\xi, \quad B_\alpha^{(n)} = \int h^{(eq)} H_\alpha^{(n)}(\hat{\xi}) d\xi. \quad (30)$$

As seen in Appendix A, the derivation of the hydrodynamic equations at the Navier-Stokes level from the kinetic model proposed in Sec. II requires the zeroth- through third-order moments of $f^{(eq)}$ and zeroth- through second-order moments of $h^{(eq)}$. Therefore, in order to obtain the same equations at the Navier-Stokes level, it is necessary to keep the terms up to third order in the Hermite expansion of $f^{(eq)}$, and to second order in the expansion of $h^{(eq)}$. With these coefficients, the truncated Hermite expansions of $f^{(eq)}$ and $h^{(eq)}$ can be written as

$$f^{(eq),3}(T) = \omega(\xi, T) \rho \left\{ 1 + \frac{\xi \cdot \mathbf{u}}{RT} + \frac{1}{2} \left(\frac{\xi \cdot \mathbf{u}}{RT} \right)^2 - \frac{u^2}{2RT} + \frac{\xi \cdot \mathbf{u}}{6RT} \left[\left(\frac{\xi \cdot \mathbf{u}}{RT} \right)^2 - \frac{3u^2}{RT} \right] \right\}, \quad (31)$$

$$h^{(eq),2}(T) = \omega(\xi, T) \left\{ \rho E + (p + \rho E) \frac{\xi \cdot \mathbf{u}}{RT} + \frac{p}{2} \left(\frac{\xi^2}{RT} - D \right) + \left(p + \frac{\rho E}{2} \right) \left[\left(\frac{\xi \cdot \mathbf{u}}{RT} \right)^2 - \frac{u^2}{RT} \right] \right\}, \quad (32)$$

For low Mach flows, the third-order term in $f^{(eq),3}$ can be neglected, and we can use the truncated expansions of $f^{(eq)}$ and $h^{(eq)}$ up to the second order, i.e.,

$$f^{(eq),2}(T) = \omega(\xi, T) \rho \left[1 + \frac{\xi \cdot \mathbf{u}}{RT} + \frac{1}{2} \left(\frac{\xi \cdot \mathbf{u}}{RT} \right)^2 - \frac{u^2}{2RT} \right], \quad (33a)$$

$$h^{(eq),2}(T) = \omega(\xi, T) \rho \left[\frac{\xi \cdot \mathbf{u}}{RT} + \left(\frac{\xi \cdot \mathbf{u}}{RT} \right)^2 - \frac{u^2}{RT} + \frac{1}{2} \left(\frac{\xi^2}{RT} - D \right) \right] + E f^{(eq),2}. \quad (33b)$$

Accordingly, the terms associated with the external force \mathbf{a} in the kinetic model (18), $\mathbf{a} \cdot \nabla_\xi f$ and $\mathbf{a} \cdot \nabla_\xi h$, should also be projected on to the Hermite basis. The Chapman-Enskog analysis of the kinetic model [see Eqs. (A10) and (A11) in Appendix A] indicates that, in order to obtain the exact Navier-Stokes equations, it is adequate to truncate the Hermite expansions of the two terms up to the second order and first order, respectively. With this in mind, after some standard manipulations we obtain

$$\mathbf{a} \cdot \nabla_\xi f = -\omega(\xi, T) \rho \left(\frac{\xi \cdot \mathbf{a}}{RT} + \frac{(\xi \cdot \mathbf{a})(\xi \cdot \mathbf{u})}{(RT)^2} - \frac{\mathbf{a} \cdot \mathbf{u}}{RT} \right), \quad (34a)$$

$$\mathbf{a} \cdot \nabla_\xi h = -\omega(\xi, T) \rho E \frac{\xi \cdot \mathbf{a}}{RT}. \quad (34b)$$

It can be readily verified that the thermohydrodynamic equations corresponding to the truncated EDFs (33) and the forcing terms (34) are just the same as those for the original unexpanded ones after neglecting the terms of $O(\text{Ma})^3$ (Ma represents the Mach number).

Here, we would like to point out that if we apply the Hermite expansion to the internal energy EDF $g^{(eq)}$ in the HCD model, we can obtain the following truncated expansion up to the second order:

$$g^{(eq),2} = \rho \epsilon \omega(\xi) \left[\frac{\xi \cdot \mathbf{u}}{RT} + \frac{1}{2} \left(\frac{\xi \cdot \mathbf{u}}{RT} \right)^2 - \frac{u^2}{2RT} + \frac{\xi^2}{DRT} \right] = \epsilon f^{(eq),2} + \rho \epsilon \omega(\xi) \left(\frac{\xi^2}{DRT} - 1 \right), \quad (35)$$

which is similar to those given in Refs. [9,13] which are obtained by regrouping the Taylor expansion of $g^{(eq)}$ heuristically.

B. Discretization of the velocity space

The discrete velocity set can be obtained by choosing the abscissae of a suitable Gauss-Hermite quadrature with the weight function $\omega(\xi, T)$ so that the required velocity moments of the truncated $f^{(eq)}$ can be exactly evaluated. However, it is noted that the temperature appearing in the truncated EDFs is a locally changed variable, which means that the abscissae of the Gauss-Hermite quadrature are not fixed. The discrete velocities obtained in this way, say $\xi_i(\mathbf{x}, t)$, will also depend on the local temperature and may change from position to position. As such, the resultant DVM cannot be consistent with the original kinetic model where the continuous particle velocity ξ is independent of time and space. As a result, we cannot derive the correct thermohydrodynamic equations because of the incommutability of ξ_i and the temporal and spatial gradients.

In order to overcome this difficulty, we replace the local temperature T in the truncated EDFs with a reference tem-

perature T_0 , just like the strategy adopted in the HCD model [9]. With this replacement, the EDFs for the VDF and TEDF now become

$$f^{(eq),2}(T_0) = \omega(\boldsymbol{\xi}, T_0) \rho \left[1 + \frac{\boldsymbol{\xi} \cdot \mathbf{u}}{RT_0} + \frac{1}{2} \left(\frac{\boldsymbol{\xi} \cdot \mathbf{u}}{RT_0} \right)^2 - \frac{u^2}{2RT_0} \right], \quad (36a)$$

$$h^{(eq),2}(T_0) = \omega(\boldsymbol{\xi}, T_0) p_0 \left[\frac{\boldsymbol{\xi} \cdot \mathbf{u}}{RT_0} + \left(\frac{\boldsymbol{\xi} \cdot \mathbf{u}}{RT_0} \right)^2 - \frac{u^2}{RT_0} + \frac{1}{2} \left(\frac{\boldsymbol{\xi}^2}{RT_0} - D \right) \right] + E f^{(eq),2}(T_0), \quad (36b)$$

where $\omega(\boldsymbol{\xi}, T_0) = (2\pi RT_0)^{-D/2} \exp(-\boldsymbol{\xi}^2/2RT_0)$ and $p_0 = \rho RT_0$. Accordingly, the local temperature T appearing in the forcing terms is also replaced with T_0 :

$$\mathbf{a} \cdot \nabla_{\boldsymbol{\xi}} f = -\omega(\boldsymbol{\xi}, T_0) \rho \left[\frac{\boldsymbol{\xi} \cdot \mathbf{a}}{RT_0} + \frac{(\boldsymbol{\xi} \cdot \mathbf{a})(\boldsymbol{\xi} \cdot \mathbf{u})}{(RT_0)^2} - \frac{\mathbf{a} \cdot \mathbf{u}}{RT_0} \right], \quad (37a)$$

$$\mathbf{a} \cdot \nabla_{\boldsymbol{\xi}} h = -\omega(\boldsymbol{\xi}, T_0) \rho E \frac{\boldsymbol{\xi} \cdot \mathbf{a}}{RT_0}. \quad (37b)$$

But notice that the temperature appearing in the total energy E is still the local value: $E = c_v T + |\mathbf{u}|^2/2$.

It is easy to verify that the zeroth- and first-order moments of $f^{(eq),2}(T_0)$ and the zeroth-order moment of $h^{(eq),2}(T_0)$ are the same as those of the EDFs with the local temperature T given by Eq. (33), i.e.,

$$\int f^{(eq),2}(T_0) d\boldsymbol{\xi} = \rho, \quad \int \boldsymbol{\xi} f^{(eq),2}(T_0) d\boldsymbol{\xi} = \rho \mathbf{u}, \quad (38a)$$

$$\int h^{(eq),2}(T_0) d\boldsymbol{\xi} = \rho E. \quad (38b)$$

The higher moments required in the derivation of the Navier-Stokes equations, however, are different because of the replacement of T with T_0 :

$$\int \xi_\alpha \xi_\beta f^{(eq),2}(T_0) d\boldsymbol{\xi} = \rho u_\alpha u_\beta + p_0 \delta_{\alpha\beta}, \quad (39a)$$

$$\int \xi_\alpha \xi_\beta \xi_\gamma f^{(eq),2}(T_0) d\boldsymbol{\xi} = p_0 (u_\alpha \delta_{\beta\gamma} + u_\beta \delta_{\alpha\gamma} + u_\gamma \delta_{\alpha\beta}), \quad (39b)$$

$$\int \xi_\alpha h^{(eq),2}(T_0) d\boldsymbol{\xi} = (p_0 + \rho E) u_\alpha, \quad (39c)$$

$$\int \xi_\alpha \xi_\beta h^{(eq),2}(T_0) d\boldsymbol{\xi} = p_0 (RT_0 + E) \delta_{\alpha\beta} + (2p_0 + \rho E) u_\alpha u_\beta. \quad (39d)$$

Based on the two modified EDFs given by Eq. (36), we can now determine the discrete velocity set easily from cer-

tain Gauss-Hermite quadratures with the weight function $\omega(\boldsymbol{\xi}, T_0)$. The quadrature should be accurate enough so that the velocity moments (38) and (39) can be evaluated exactly. For $f^{(eq),2}(T_0)$, since the third-order velocity moment needs to be evaluated accurately in order to obtain the hydrodynamic equations at the Navier-Stokes order, a Gauss-Hermite quadrature with at least the fifth degree of precision is required [notice that $f^{(eq),2}(T_0)$ itself contains second-order terms of $\boldsymbol{\xi}$]. For $h^{(eq),2}(T_0)$, on the other hand, a Gauss-Hermite quadrature with at least the fourth degree of precision is required because the second-order moment needs to be evaluated exactly in the derivation of the energy equation. Therefore, a Gauss-Hermite quadrature with the fifth degree of precision can be chosen to determine the discrete velocity set for the kinetic model with the modified EDFs (36). For the two-dimensional case, we can choose the nine-point fifth-degree Gauss-Hermite quadrature, which leads to the following discrete velocities (D2Q9 model):

$$\mathbf{c}_i = \begin{cases} (0, 0) & i = 0, \\ c \left(\cos\left((i-1)\frac{\pi}{2}\right), \sin\left((i-1)\frac{\pi}{2}\right) \right), & i = 1, 2, 3, 4, \\ c \left(\cos\left(\left(i-\frac{9}{2}\right)\frac{\pi}{2}\right), \sin\left(\left(i-\frac{9}{2}\right)\frac{\pi}{2}\right) \right), & i = 5, 6, 7, 8, \end{cases}$$

where $c = \sqrt{3RT_0}$. The weight coefficients corresponding to these velocities are $w_0 = 4/9$, $w_1 = w_2 = w_3 = w_4 = 1/9$, and $w_5 = w_6 = w_7 = w_8 = 1/36$. Similarly, for three-dimensional case we can obtain the 15-velocity (D3Q15) and 19-velocity (D3Q19) models [33].

Once the abscissa of the Gauss-Hermite quadrature is chosen, the integral of a function of $\boldsymbol{\xi}$, say ϕ , can be evaluated as

$$\int \omega(\boldsymbol{\xi}, T_0) \phi(\boldsymbol{\xi}) d\boldsymbol{\xi} = \sum_{i=1}^b w_i \phi(\mathbf{c}_i), \quad (40)$$

where $\{\mathbf{c}_i | i=1, 2, \dots, b\}$ is the abscissa and w_i is the quadrature weight. Therefore, if we define

$$f_i(\mathbf{x}, t) = \frac{w_i f(\mathbf{x}, \mathbf{c}_i, t)}{\omega(\mathbf{c}_i, T_0)}, \quad h_i(\mathbf{x}, t) = \frac{w_i h(\mathbf{x}, \mathbf{c}_i, t)}{\omega(\mathbf{c}_i, T_0)},$$

we can evaluate the integrals in Eq. (20) or Eq. (28) using the quadrature and determine the fluid variables as

$$\rho = \sum_i f_i, \quad \rho \mathbf{u} = \sum_i \mathbf{c}_i f_i, \quad \rho E = \sum_i h_i. \quad (41)$$

The evolution equations for the reduced distribution functions f_i and h_i can be easily derived from the kinetic equations (18) for f and h , which lead to the following discrete velocity model;

$$\partial_t f_i + \mathbf{c}_i \cdot \nabla f_i = -\frac{1}{\tau_f}(f_i - f_i^{(eq)}) + F_i, \quad (42a)$$

$$\partial_t h_i + \mathbf{c}_i \cdot \nabla h_i = -\frac{1}{\tau_h}(h_i - h_i^{(eq)}) + \frac{Z_i}{\tau_{hf}}(f_i - f_i^{(eq)}) + q_i, \quad (42b)$$

where $Z_i = \mathbf{c}_i \cdot \mathbf{u} - u^2/2$, and

$$f_i^{(eq)} = w_i \rho \left[1 + \frac{\mathbf{c}_i \cdot \mathbf{u}}{RT_0} + \frac{1}{2} \left(\frac{\mathbf{c}_i \cdot \mathbf{u}}{RT_0} \right)^2 - \frac{u^2}{2RT_0} \right], \quad (43a)$$

$$h_i^{(eq)} = w_i p_0 \left[\frac{\mathbf{c}_i \cdot \mathbf{u}}{RT_0} + \left(\frac{\mathbf{c}_i \cdot \mathbf{u}}{RT_0} \right)^2 - \frac{u^2}{RT_0} + \frac{1}{2} \left(\frac{\mathbf{c}_i^2}{RT_0} - D \right) \right] + E f_i^{(eq)}, \quad (43b)$$

F_i and q_i are two terms related to the external force:

$$F_i = w_i \rho \left(\frac{\mathbf{c}_i \cdot \mathbf{a}}{RT_0} + \frac{(\mathbf{c}_i \cdot \mathbf{a})(\mathbf{c}_i \cdot \mathbf{u})}{(RT_0)^2} - \frac{\mathbf{a} \cdot \mathbf{u}}{RT_0} \right), \quad (44a)$$

$$q_i = w_i \rho E \frac{\mathbf{c}_i \cdot \mathbf{a}}{RT_0} + f_i \mathbf{c}_i \cdot \mathbf{a}. \quad (44b)$$

Through the Chapman-Enskog analysis, the thermohydrodynamic equations corresponding to the DVM (42) can be derived at the Navier-Stokes level as (see Appendix B):

$$\partial_t \rho + \nabla \cdot (\rho \mathbf{u}) = 0, \quad (45a)$$

$$\partial_t (\rho \mathbf{u}) + \nabla \cdot (\rho \mathbf{u} \mathbf{u}) = -\nabla p_0 + \nabla \cdot \boldsymbol{\tau} + \rho \mathbf{a}, \quad (45b)$$

$$\partial_t (\rho E) + \nabla \cdot [(\rho_0 + \rho E) \mathbf{u}] = \nabla \cdot (\lambda \nabla T) + \nabla \cdot (\boldsymbol{\tau} \cdot \mathbf{u}) + \rho \mathbf{u} \cdot \mathbf{a}, \quad (45c)$$

where $p_0 = \rho R T_0$, $\boldsymbol{\tau} = \mu \mathbf{S}$, $\mu = \tau_f p_0$, and $\lambda = c_v \tau_h p_0$.

Although Eqs. (45) look similar to those derived from the original kinetic model, i.e., Eqs. (21), the following differences between them should be noticed. First, the equation of state and the transport coefficients in Eqs. (45) depend only on the reference temperature T_0 , while those in Eqs. (21) depend on the local temperature. In other words, the thermohydrodynamic equations (21) are fully coupled, while in Eqs. (45) the energy equation is decoupled from the momentum equation since it can be solved independently once the first two equations are solved. In this sense, the DVM (42) can be termed a *decoupled* DVM. The second difference lies in the viscous stress tensor $\boldsymbol{\tau}$. In Eqs. (45) the trace of $\boldsymbol{\tau}$ is nonzero, which means that the bulk viscosity is also nonzero and equal to $2\mu/D$. On the contrary, in (21) the viscous stress is traceless and the bulk viscosity is zero. The final difference appears in the thermal conductivity: in Eqs. (21) it is given by $\lambda = c_p \tau_h p$, but in Eqs. (45) it is given by $\lambda = c_v \tau_h p$. Therefore, for the DVM the two relaxation times are related to the Prandtl number as $\text{Pr} = \mu c_p / \lambda = \gamma \tau_f / \tau_h$, which is different from the result of the continuous kinetic model.

IV. THERMAL LATTICE BOLTZMANN MODEL

A. Lattice Boltzmann equations

Base on the DVM presented in the above section, we can construct a thermal LBE model for low Mach flows by discretizing the temporal and spatial derivatives following some standard procedures. First, the time discretization for Eq. (42a) can be made by integrating the equation along the characteristic line, which leads to

$$\begin{aligned} f_i(\mathbf{x} + \mathbf{c}_i \delta_t, t + \delta_t) - f_i(\mathbf{x}, t) \\ = \int_0^{\delta_t} [\Omega_f(\mathbf{x} + \mathbf{c}_i t', t + t') + F_i(\mathbf{x} + \mathbf{c}_i t', t + t')] dt', \end{aligned} \quad (46)$$

where δ_t is the time step and $\Omega_f = (f_i^{(eq)} - f_i) / \tau_f$. As argued in Ref. [9], the integral on the right-hand side must be evaluated with at least second-order accuracy. The trapezoidal rule can serve this purpose and leads to the following time-discrete scheme:

$$\begin{aligned} f_i(\mathbf{x} + \mathbf{c}_i \delta_t, t + \delta_t) - f_i(\mathbf{x}, t) \\ = \frac{\delta_t}{2} [\Omega_f(\mathbf{x} + \mathbf{c}_i \delta_t, t + \delta_t) + F_i(\mathbf{x} + \mathbf{c}_i \delta_t, t + \delta_t)] \\ + \frac{\delta_t}{2} [\Omega_f(\mathbf{x}, t) + F_i(\mathbf{x}, t)]. \end{aligned} \quad (47)$$

As suggested by He *et al.* [9], the implicitness of the above scheme can be eliminated by introducing the following distribution function:

$$\bar{f}_i = f_i - \frac{\delta_t}{2} (\Omega_f + F_i), \quad (48)$$

from which one can obtain

$$f_i - f_i^{(eq)} = \left(1 + \frac{\delta_t}{2\tau_f} \right)^{-1} \left(\bar{f}_i - f_i^{(eq)} + \frac{\delta_t}{2} F_i \right) \quad (49)$$

and

$$\bar{f}_i - f_i = -\frac{\delta_t}{2} (\Omega_f + F_i). \quad (50)$$

With the aids of Eqs. (49) and (50), Eq. (47) can be rewritten as

$$\begin{aligned} \bar{f}_i(\mathbf{x} + \mathbf{c}_i \delta_t, t + \delta_t) - \bar{f}_i(\mathbf{x}, t) \\ = -\omega_f [\bar{f}_i(\mathbf{x}, t) - f_i^{(eq)}(\mathbf{x}, t)] + \delta_t \left(1 - \frac{\omega_f}{2} \right) F_i, \end{aligned} \quad (51)$$

where $\omega_f = 2\delta_t / (2\tau_f + \delta_t)$. From Eq. (48), it can be easily verified that the density and velocity of the fluid can be computed from the new VDF as

$$\rho = \sum_i \bar{f}_i, \quad \rho \mathbf{u} = \sum_i \mathbf{c}_i \bar{f}_i + \frac{\delta_t}{2} \rho \mathbf{a}. \quad (52)$$

It is noted that the treatment of the forcing term in Eq. (51) is just the same as that proposed in [34].

The discrete kinetic equation (42b) can be discretized using a similar approach. Specifically, the use of characteristic discretization and trapezoidal quadrature leads to the following implicit scheme:

$$h_i(\mathbf{x} + \mathbf{c}_i \delta_t, t + \delta_t) - h_i(\mathbf{x}, t) = \int_0^{\delta_t} [\Omega_h(\mathbf{x} + \mathbf{c}_i t', t + t') + S_i(\mathbf{x} + \mathbf{c}_i t', t + t')] dt', \quad (53)$$

where $S_i = Z_i \Omega_f / \tau_{hf} + q_i$. The implicitness can be eliminated by introducing the following energy DF:

$$\bar{h}_i = h_i - \frac{\delta_t}{2} (\Omega_h + S_i), \quad (54)$$

from which one can obtain

$$h_i - h_i^{(eq)} = \left(1 + \frac{\delta_t}{2\tau_h}\right)^{-1} \left(\bar{h}_i - h_i^{(eq)} + \frac{\delta_t}{2} S_i\right) \quad (55)$$

and

$$\bar{h}_i - h_i = -\frac{\delta_t}{2} (\Omega_h + S_i). \quad (56)$$

Therefore, the LBE for this energy DF is now

$$\begin{aligned} \bar{h}_i(\mathbf{x} + \mathbf{c}_i \delta_t, t + \delta_t) - \bar{h}_i(\mathbf{x}, t) &= \delta_t (\Omega_h + S_i) = -\omega_h [\bar{h}_i(\mathbf{x}, t) - h_i^{eq}(\mathbf{x}, t)] + \delta_t \left(1 - \frac{\omega_h}{2}\right) S_i \\ &= -\omega_h [\bar{h}_i(\mathbf{x}, t) - h_i^{eq}(\mathbf{x}, t)] + \delta_t \left(1 - \frac{\omega_h}{2}\right) q_i \\ &\quad + \delta_t \left(1 - \frac{\omega_h}{2}\right) \frac{Z_i}{\tau_{hf}} (f_i - f_i^{(eq)}), \end{aligned} \quad (57)$$

where $\omega_f = 2\delta_t / (2\tau_f + \delta_t)$.

The underlined term in the above equation can be further rewritten in terms of the VDF \bar{f}_i . In fact, by noticing that $\tau_f = \delta_t (\omega_f^{-1} - 0.5)$ and $\tau_h = \delta_t (\omega_h^{-1} - 0.5)$, we can obtain that

$$\frac{1}{\tau_{hf}} \left(1 + \frac{\delta_t}{2\tau_f}\right)^{-1} = \frac{\omega_h - \omega_f}{\delta_t (1 - \omega_h/2)}. \quad (58)$$

Therefore, after substituting the expression (49), the underlined term becomes

$$(\omega_h - \omega_f) Z_i \left(\bar{f}_i - f_i^{(eq)} + \frac{\delta_t}{2} F_i \right). \quad (59)$$

As a result, the final formulation of the time-discrete scheme for the energy equation can be written as

$$\begin{aligned} \bar{h}_i(\mathbf{x} + \mathbf{c}_i \delta_t, t + \delta_t) - \bar{h}_i(\mathbf{x}, t) &= -\omega_h [\bar{h}_i(\mathbf{x}, t) - h_i^{eq}(\mathbf{x}, t)] + \delta_t \left(1 - \frac{\omega_h}{2}\right) q_i \\ &\quad + (\omega_h - \omega_f) Z_i \left(\bar{f}_i - f_i^{(eq)} + \frac{\delta_t}{2} F_i \right), \end{aligned} \quad (60)$$

and the total energy can now be determined by

$$\rho E = \sum_i \bar{h}_i + \frac{\delta_t}{2} \rho \mathbf{u} \cdot \mathbf{a}. \quad (61)$$

After the time is discretized, we now arrive at another key point for constructing the LBE, i.e., the discretization of the space. In a standard LBE model, the spatial space is discretized into a regular lattice \mathcal{L} with a spacing such that, for a node $\mathbf{x} \in \mathcal{L}$, the point $\mathbf{x} + \mathbf{c}_i \delta_t$ is the nearest lattice point of \mathbf{x} along the direction \mathbf{c}_i . This means that, if a particle moving with a discrete velocity is located on the lattice, it will jump to the nearest neighbor on the lattice in the next step. For instance, in the D2Q9 model the lattice spacing is chosen to be $\delta_x = c \delta_t$ with $c = \sqrt{3RT_0}$. Therefore, the lattice is closely dependent on the discrete velocity set, meaning that the spatial discretization is coupled with the velocity discretization.

With the time integration and the space discretization, the two discrete kinetic equations (51) and (60) become fully discrete now, and they constitute our decoupling thermal LBE model for low Mach number flows. The present LBE model can also be easily extended to polyatomic gases by simply changing the specific heat c_v from $DR/2$ to $(D+K)R/2$.

It can be easily shown that the thermohydrodynamic equations derived from the LBE model are just those of the DVM, i.e., (45). Therefore, theoretically the present LBE model is applicable only to Boussinesq flows where the sound speed and the transport coefficients are independent of temperature. It is also because of this fact that we call the model a decoupling one. However, from the computational point of view, the restriction on the transport coefficients can be released to some extent. That is, if we know the relation between these coefficients and the local temperature in advance, we can make τ_f and τ_h functions of temperature,

$$\tau_f = \frac{\mu(T)}{p_0} \quad \text{and} \quad \tau_h = \frac{\lambda(T)}{c_v p_0}.$$

With such modifications, the LBE model can also be applied to flows with temperature-dependent transport coefficients.

It is also interesting to make a comparison between the present LBE model and the HCD model [9]. First, it is noted that both models share many similar features: the low Mach number limit, the replacement of local temperature with a reference one in the EDFs, and the decoupling between the momentum and energy equations. On the other hand, the differences between the two models are also apparent: the HCD model uses the internal energy distribution, while the present model employs the total energy distribution. As a result of this different choice, the HCD model contains a complicated differential term that needs special treatment, while the present model is able to avoid such difficulty.

B. Some special cases

1. Flows with negligible compression work and viscous dissipation

In many practical applications, compression work and viscous heat can be neglected. The present LBE model can be

easily applied to such problems by simply taking $c_p = c_v \rightarrow \infty$ in the model. This can be seen more clearly if we rewrite the energy equation (45c) in nondimensional form as

$$\partial_t(\rho\theta) + \nabla \cdot (\rho\mathbf{u}\theta) = \nabla \cdot \left(\frac{\gamma}{\text{Pr Re}} \nabla \theta \right) - \gamma \text{Ec} \rho_0 \nabla \cdot \mathbf{u} + \frac{\gamma \text{Ec}}{\text{Re}} \mathbf{S} : \nabla \mathbf{u}, \quad (62)$$

where $\theta = (T - T_0)/\Delta T$, with T_0 and ΔT being the characteristic temperature and temperature variation. The parameters $\text{Pr} = c_p \mu / \lambda$, $\text{Re} = Lu_0 / \nu$, and $\text{Ec} = u_0^2 / c_p \Delta T$ are the Prandtl number, Reynolds number, and Eckert number, respectively, with L being the characteristic length and u_0 the characteristic velocity. $\gamma = c_p / c_v$ is the ratio of the specific heats, which can be taken to be unity for incompressible fluids. As c_p is large enough, the Eckert number will become sufficient small so that the compression work and the viscous heat dissipation terms are negligible.

It is noted that, for the HCD model, the evolution equations should also be modified if compression work and viscous heat are neglected [9]. However, despite the neglect of the two factors, a complicated gradient term similar to that in the original HCD model still exists in the modified HCD model.

2. Flows with buoyancy force

In natural convection and mixed-convection flows, the buoyancy force should be considered. As the temperature difference ΔT is small in comparison with the average temperature T_0 , the Boussinesq assumption can be invoked. That is, the fluid properties are assumed to be independent of the temperature, except that the density in the gravitational force is assumed to be

$$\rho = \rho_0 [1 - \beta(T - T_0)], \quad (63)$$

where ρ_0 is the fluid density at temperature T_0 and β is the thermal expansion coefficient. As such, the gravity force can be expressed as

$$\rho \mathbf{g} = \rho_0 \mathbf{g} - \rho_0 \beta (T - T_0), \quad (64)$$

where \mathbf{g} is the acceleration due to gravity. After absorbing the constant part $\rho_0 \mathbf{g}$ into the pressure, the effective external force becomes

$$\rho \mathbf{a} = -\rho_0 \beta (T - T_0).$$

However, it should be noted that, with this effective force, the pressure field modeled by the LBE is actually the dynamic part, $p' = p_0 - \rho_0 g y$, with g being the magnitude of the gravity and y the coordinate opposite to the gravity force. With such a treatment, the work done by the pressure that enters the energy equation contains only the dynamic part. In other words, the momentum and energy equations corresponding to the LBE are actually

$$\partial_t(\rho' \mathbf{u}) + \nabla \cdot (\rho' \mathbf{u} \mathbf{u}) = -\nabla p' + \nabla \cdot \boldsymbol{\tau} + \rho' \mathbf{a}, \quad (65a)$$

$$\partial_t(\rho' E) + \nabla \cdot [(p' + \rho' E) \mathbf{u}] = \nabla \cdot (\lambda \nabla T) + \nabla \cdot (\boldsymbol{\tau} \cdot \mathbf{u}) + \rho' \mathbf{u} \cdot \mathbf{a}, \quad (65b)$$

with $p' = \rho' R T_0$ the dynamic pressure and $\rho' \approx \rho_0$ the corresponding fluid density. As the compression work is negligible, such a treatment can work well. On the other hand, when the compression work plays an important role, the total pressure should be used in the energy equation for the sake of thermodynamic consistency [38]. In order to account for this effect, we include the work done by the static pressure into the term q_i in the LBE (60),

$$q_i = (w_i \rho' E R T_0 + f_i) \mathbf{c}_i \cdot \mathbf{a} + \omega_i \rho' \mathbf{u} \cdot \mathbf{g}. \quad (66)$$

Accordingly, the total energy is calculated by

$$\rho' E = \sum_i \bar{h}_i + \frac{\delta_i}{2} \rho' \mathbf{u} \cdot (\mathbf{a} + \mathbf{g}). \quad (67)$$

One can show that with the modified q_i the energy equation corresponding to the LBE model is

$$\rho' c_v (\partial_t T + \mathbf{u} \cdot \nabla T) = \nabla \cdot (\lambda \nabla T) - p' \nabla \cdot \mathbf{u} + \boldsymbol{\tau} : \nabla \mathbf{u} + \rho' \mathbf{u} \cdot \mathbf{g}, \quad (68)$$

which is similar to that in Ref. [38] in the incompressible limit (i.e., $\rho' \approx \rho_0$).

C. Boundary conditions

In practical applications, the flow boundary conditions are usually specified in terms of the fluid variables. In order to transform thermohydrodynamic boundary conditions to the boundary conditions for the distribution functions, we employ the nonequilibrium-extrapolation approach in this work due to its simplicity, second-order accuracy, and good robustness [35]. The approach was originally proposed to realize plane boundaries for isothermal LBEs. Recently, this approach has been extended to curve boundaries [36] and to TLBEs [11,37].

The basic idea of the nonequilibrium extrapolation approach is to separate a DF at a boundary node into its equilibrium and nonequilibrium parts, where the hydrodynamic boundary conditions are enforced through the equilibrium, and the nonequilibrium part is approximated by that of the DF at the nearest neighbor node in the fluid region. Following this approach, the density DF \bar{f}_i at a boundary node \mathbf{x}_b can be specified as

$$\bar{f}_i(\mathbf{x}_b) = f_i^{(eq)}(\mathbf{x}_b, \rho_b, \mathbf{u}_b) + [\bar{f}_i(\mathbf{x}_f) - f_i^{(eq)}(\mathbf{x}_f)], \quad (69)$$

where \mathbf{x}_f is the nearest fluid neighborhood. For the velocity boundary condition where the velocity \mathbf{u}_b is known, ρ_b is just a parameter, not necessarily equal to the density at \mathbf{x}_b . It has been demonstrated that it is a good approximation to set $\rho_b = \rho(\mathbf{x}_f)$ [11,35,36]. Similarly, for thermal boundary conditions where the temperature at the boundary is known, the energy DF h_i is approximated as

$$\bar{h}_i(\mathbf{x}_b) = h_i^{(eq)}(\mathbf{x}_b, \rho_b, E_b) + [\bar{h}_i(\mathbf{x}_f) - h_i^{(eq)}(\mathbf{x}_f)], \quad (70)$$

where $E_b = c_v T_b + \mathbf{u}_b^2 / 2$. It is noted that, if the heat flux $\dot{q} = \partial T / \partial \mathbf{n}$ is specified at the boundary, with \mathbf{n} being the unit

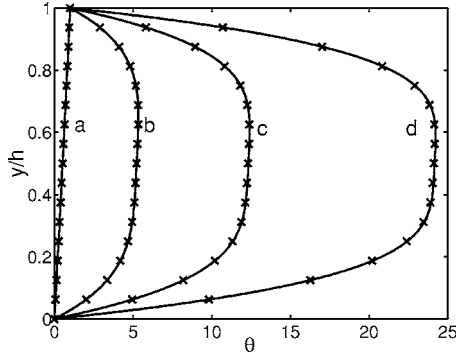


FIG. 1. Temperature variation $[\theta=(T-T_c)/(T_h-T_c)]$ of the thermal Poiseuille flow at $Re=20$ and $Pr=0.71$. (a)–(d) $Ec=0.1, 20, 50,$ and 100 . Solid lines are the analytical solutions, and the symbols are the numerical results.

vector normal to the boundary, the energy DF can also be approximated according to Eq. (70), except that T_b is now given by some numerical schemes of the heat flux.

V. NUMERICAL TESTS

A number of simulations, including the planar thermal Poiseuille flow and the natural convection in a square cavity, have been carried out to validate the present thermal LBE model. In the simulations, the two-dimensional nine-speed (D2Q9) model is employed.

A. Planar thermal Poiseuille flow

The thermal Poiseuille flow in a planar channel considered here is driven by a constant force a , and the temperature of the bottom and top walls of the channel are kept at T_h and T_c , respectively. If the gravity is neglected, the velocity and the temperature profiles can be described as

$$u(y) = 4u_0y^*(1 - y^*), \tag{71a}$$

$$\theta = y^* + \frac{PrEc}{3}[1 - (1 - 2y^*)^4], \tag{71b}$$

where $y^*=y/h$ (h being the channel height), $u_0=\rho_0ah^2/8\mu$, and $\theta=(T-T_c)/(T_h-T_c)$.

The thermal Poiseuille flow is characterized by the Reynolds number $Re=\rho_0hu_0/\mu$, the Prandtl number $Pr=\mu c_p/\lambda$, and the Eckert number $Ec=u_0^2/c_p(T_h-T_c)$. We carried out a set of simulations for different values of Re , Pr , and Ec . The specific heat ratio γ is set to be unity since the flow can be considered to be incompressible. In our simulations, a 64×64 lattice is employed, and the nonequilibrium extrapolation method is used to treat velocity and temperature boundary conditions for the bottom and top walls (69) and (70). In the streamwise (x) direction, periodic boundary conditions are applied to the inlet and outlet. In our simulations the Reynolds number is taken to be $Re=20$ and the maximum velocity u_0 is set to be 1.0. The relaxation parameter ω_f is set to be 0.8 so that the computational Mach number $u_0/\sqrt{3RT_0}$ is about 0.08, which ensures the low Mach number require-

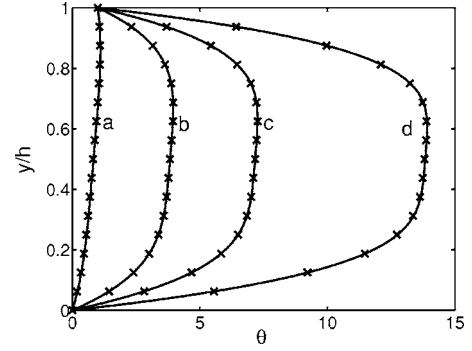


FIG. 2. Temperature variation $[\theta=(T-T_c)/(T_h-T_c)]$ of the thermal Poiseuille flow at $Re=20$ and $Ec=10.0$. (a)–(d) $Pr=0.1, 1.0, 2.0,$ and 4.0 . Solid lines are the analytical solutions, and the symbols are the numerical results.

ment. Other parameters can be determined from the non-dimensional parameters.

The temperature profiles for $Pr=0.71$ as Ec varies from 0.1 to 100 are presented in Fig. 1, while the temperature profiles for a fixed Eckert number ($Ec=10$) as Pr varies from 0.1 to 4 are shown in Fig. 2. It is clearly seen that the numerical results are in excellent agreement with the analytical solutions. The viscous heat effects are successfully captured by the present thermal LBE model over a wide range of the product of Pr and Ec .

It is known that a thermal LBE usually loses stability or accuracy as ω_f and/or ω_h approach to 2.0 or when the temperature variation is large. In order to demonstrate the range of applicability of the present model, we test the model by varying the two relaxations times τ_f and τ_h , and the temperature difference $(T_h-T_c)/T_c$. In the simulations the driven force is chosen such that the maximum velocity $u_0=0.1c$, with the 64×64 lattice. It is found that the LBE is still stable and accurate in both velocity and temperature even when both τ_f/δ_t and τ_h/δ_t are as small as 10^{-4} when $(T_h-T_c)/T_c$ ranges from 0 to 1000. It is clear that applicability range and numerical stability of the present LBE are similar to those of the HCD model [9] and are much wider and better than those of the multispeed LBE model [5].

B. Natural convection in a square cavity

We now apply the thermal LBE model to the natural convection flow in a two-dimensional square cavity. The two sidewalls (left and right) of the cavity are maintained at two different temperatures T_c and T_h ($T_h > T_c$), respectively, while the bottom and top walls are adiabatic. The convection flow induced by the temperature difference is characterized by the Prandtl number Pr and Rayleigh number $Ra = \rho_0^2 c_p g \beta \Delta T H^3 / \mu \lambda$, where ρ_0 is the reference density, $\Delta T = T_h - T_c$ is the temperature difference between the hot and cool walls, and H is the height of the cavity.

We first simulated the natural convection problem with negligible compression work and heat dissipation. This is achieved by setting the Eckert number to be as small as 10^{-30} . The Prandtl number is set to be 0.71, and the Rayleigh number ranges from 10^3 to 10^6 . In the computations a 128

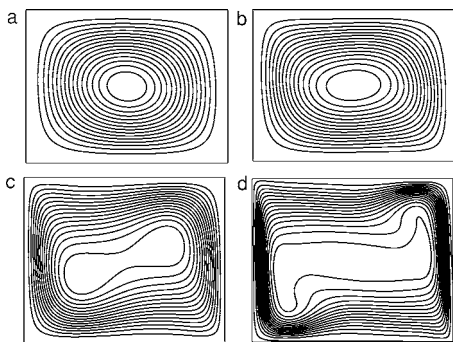


FIG. 3. Streamlines for $Ra=10^3$ (a), 10^4 (b), 10^5 (c), and 10^6 (d) of the natural convection flow in a cavity.

$\times 128$ lattice is employed and the relaxation parameter w_f is chosen to be 1.6 for all cases. The nonequilibrium extrapolation method is applied to specify the boundary conditions for both the density DF f_i and the energy DF h_i at the four solid walls.

Streamlines and isotherm lines predicted by the present TLBE model are shown in Figs. 3 and 4. It is seen that for low Ra a central vortex appears as a typical feature of the flow. The vortex tends to become elliptic as Ra increases, and breaks up into two vortices at $Ra=10^5$. As Ra reaches 10^6 , the two vortices move toward the walls and a third vortex appears in the center of the cavity. The isotherm lines indicate the change of the dominant heat transfer mechanism with Rayleigh number. For small Ra , the heat is transferred mainly by conduction between the hot and cold walls, and the isotherms are almost vertical. As Ra increases, the dominant heat transfer mechanism changes from conduction to convection, and the isotherm lines become horizontal in the center of the cavity, and are vertical only in the thin boundary layers near the hot and cold walls. All of these observations are in good agreement with results reported in previous studies [39,40].

To quantify the results, we computed the Nusselt number along the two sidewalls and the maximum velocities along the horizontal and vertical lines through the cavity center. The results are listed in Table I together with the data from previous studies. As shown, the TLBE results agree well with the available data. In fact, the difference between the present LBE results and the reference ones are within 1.0% for the cases considered.

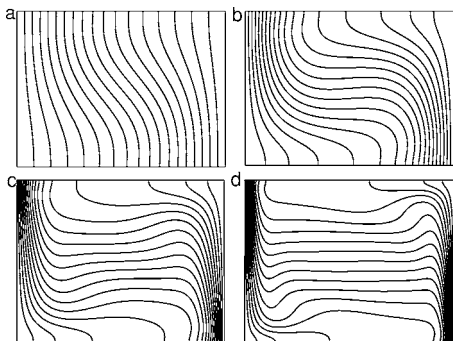


FIG. 4. Isotherm lines for $Ra=10^3$ (a), 10^4 (b), 10^5 (c), and 10^6 (d) of the natural convection flow in a cavity.

TABLE I. Comparisons of the average Nusselt number and the maximum velocity components across the cavity center. The data in parentheses are the locations of the maxima.

Ra		Nu	$u_{max}(y)$	$v_{max}(x)$
10^3	Present	1.1195	3.643 (0.8047)	3.6919 (0.1719)
	Ref. [11]	1.1168	3.6554 (0.8125)	3.6985 (0.1797)
10^4	Present	2.2545	16.1254 (0.8203)	19.5577 (0.1172)
	Ref. [39]	2.2442	16.1802 (0.8265)	19.6295 (0.1193)
10^5	Present	4.5278	34.6033 (0.8516)	68.0820 (0.0703)
	Ref. [39]	4.5216	34.7399 (0.8558)	68.6396 (0.0657)
10^6	Present	8.7746	64.9059 (0.8516)	218.900 (0.0391)
	Ref. [39]	8.8251	64.8367 (0.8505)	220.461 (0.0390)

We now examine the effects of compression work and viscous dissipation on natural convection. The Prandtl number and the Rayleigh number are set to be 1.0 and 10^5 , respectively. The size of the computational mesh is 256×256 and the relaxation parameter w_f is set to be 1.6. The temperatures of the cool and hot sidewalls are kept at 300 and 310 K, respectively. Two values of the Eckert number are used in our simulations, i.e., $Ec=10^{-30}$ and 10^{-5} , where in the former case the pressure work and viscous dissipation are neglected while in the latter case the effects are included.

In Fig. 5, the streamlines and isothermal lines are presented for comparison. It is clearly seen that the flow and heat transfer behaviors in the two cases are quite different. As compression work and viscous dissipation are considered, flow occurs only in the regions very close to the walls, and the isotherms are very dense in the near-wall region, and rather sparse in the interior region of the cavity.

The Nusselt numbers on the cool and hot walls in the two cases are also measured. As listed in Table II, the heat transfer is greatly enhanced if compression work and viscous dissipation are considered, which is consistent with the larger temperature gradients in the near-wall regions shown in Fig. 5. These results also agree well quantitatively with those reported in Ref. [38] for the same case.

VI. SUMMARY

In this paper, we have developed a thermal lattice Boltzmann equation for low-speed flows based on a two-

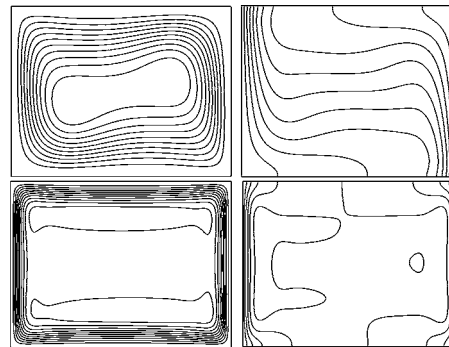


FIG. 5. Streamlines (left) and isotherms (right) for $Ra=10^5$, $Pr=1$. Top, without, and bottom, with consideration of the pressure work and viscous dissipation.

TABLE II. The average Nusselt numbers at hot (Nu_h) and cool (Nu_c) walls for $Pr=1$ and $Ra=10^5$.

Ec		Nu_h	Nu_c
10^{-30}	Present	4.6128	4.6128
10^{-5}	Present	13.1201	13.2447
	Ref. [38]	13.200	13.198

relaxation-time kinetic model. The proposed model is constructed in the DDF framework. The most distinctive feature of the present model is that an additional distribution function is defined to represent the total energy, instead of representing either the internal energy or the temperature in previous studies. This choice not only enables the final TLBE model to be simple but also makes the inclusion of compression work and viscous dissipation to be easier. The numerical tests show that the results predicted by the TLBE model are excellent agreement with the analytical solutions and numerical results reported in previous studies.

It should be pointed out that in the present model the energy equation is decoupled from the momentum equation due to the replacement of the local temperature with the constant reference temperature in the equilibrium distribution functions. Such a decoupling causes the present TLBE model to be limited to Boussinesq flows, in which the temperature variation is small, such that the transport coefficients and the sound speed become almost independent of temperature. The extension of the present TLBE model to systems in which the momentum and energy transport are coupled is under way.

ACKNOWLEDGMENTS

This work is supported by the National Basic Research Program of China (Grant No. 2006CB705804) and the National Natural Science Foundation of China (Grant No. 50606012).

APPENDIX A: CHAPMAN-ENSKOG ANALYSIS OF THE KINETIC MODEL

By introducing the following Chapman-Enskog expansions [24]:

$$\partial_t = \sum_{n=1}^{\infty} \varepsilon^n \partial_{t_n}, \quad \nabla = \varepsilon \nabla_1, \quad \mathbf{a} = \varepsilon \mathbf{a}_1, \quad (\text{A1a})$$

$$f = \sum_{n=0}^{\infty} \varepsilon^n f^{(n)}, \quad h = \sum_{n=0}^{\infty} \varepsilon^n h^{(n)}, \quad (\text{A1b})$$

where ε is a small expansion parameter, we can rewrite the kinetic equations (18) in the consecutive orders of the parameter ε as

$$\varepsilon^0: \quad f^{(0)} = f^{(eq)}, \quad (\text{A2a})$$

$$\varepsilon^1: \quad D_{t_1} f^{(0)} = -\frac{f^{(1)}}{\tau_f}, \quad (\text{A2b})$$

$$\varepsilon^2: \quad \partial_{t_2} f^{(0)} + D_{t_1} f^{(1)} = -\frac{f^{(2)}}{\tau_f}, \quad (\text{A2c})$$

and

$$\varepsilon^0: \quad h^{(0)} = h^{(eq)}, \quad (\text{A3a})$$

$$\varepsilon^1: \quad D_{t_1} h^{(0)} = -\frac{h^{(1)}}{\tau_h} + \frac{Zf^{(1)}}{\tau_{hf}} + f^{(0)} \boldsymbol{\xi} \cdot \mathbf{a}_1, \quad (\text{A3b})$$

$$\varepsilon^2: \quad \partial_{t_2} h^{(0)} + D_{t_1} h^{(1)} = -\frac{h^{(2)}}{\tau_h} + \frac{Zf^{(2)}}{\tau_{hf}} + f^{(1)} \boldsymbol{\xi} \cdot \mathbf{a}_1, \quad (\text{A3c})$$

where $D_{t_1} = \partial_{t_1} + \boldsymbol{\xi} \cdot \nabla_1 + \mathbf{a}_1 \cdot \nabla_{\boldsymbol{\xi}}$. Equations (A2a) and (A3a) indicate that

$$\int f^{(n)} d\boldsymbol{\xi} = 0, \quad \int \boldsymbol{\xi} f^{(n)} d\boldsymbol{\xi} = \mathbf{0}, \quad \int h^{(n)} d\boldsymbol{\xi} = 0 \quad (\text{A4})$$

for $n > 0$, because

$$\begin{pmatrix} \rho \\ \rho \mathbf{u} \\ \rho E \end{pmatrix} = \begin{pmatrix} \int f d\boldsymbol{\xi} \\ \int \boldsymbol{\xi} f d\boldsymbol{\xi} \\ \int h d\boldsymbol{\xi} \end{pmatrix} = \begin{pmatrix} \int f^{(eq)} d\boldsymbol{\xi} \\ \int \boldsymbol{\xi} f^{(eq)} d\boldsymbol{\xi} \\ \int h^{(eq)} d\boldsymbol{\xi} \end{pmatrix}. \quad (\text{A5})$$

Furthermore, after some standard algebra we can obtain the following results:

$$\Pi_{\alpha\beta}^{(0)} = \int \xi_{\alpha} \xi_{\beta} f^{(0)} d\boldsymbol{\xi} = p \delta_{\alpha\beta} + \rho u_{\alpha} u_{\beta}, \quad (\text{A6a})$$

$$Q_{\alpha}^{(0)} = \int \xi_{\alpha} h^{(0)} d\boldsymbol{\xi} = (p + \rho E) u_{\alpha}, \quad (\text{A6b})$$

$$\int \xi_{\alpha} \xi_{\beta} \xi_{\gamma} f^{(0)} d\boldsymbol{\xi} = p(u_{\alpha} \delta_{\beta\gamma} + u_{\beta} \delta_{\alpha\gamma} + u_{\gamma} \delta_{\alpha\beta}) + \rho u_{\alpha} u_{\beta} u_{\gamma}, \quad (\text{A6c})$$

$$\int \xi_{\alpha} \xi_{\beta} h^{(0)} d\boldsymbol{\xi} = p(RT + E) \delta_{\alpha\beta} + (2p + \rho E) u_{\alpha} u_{\beta}, \quad (\text{A6d})$$

where δ is the Kronecker delta with two indices.

From Eqs. (A2b) and (A3b), we can obtain the thermohydrodynamic equations at the first order:

$$\partial_{t_1} \rho + \nabla_1 \cdot (\rho \mathbf{u}) = 0, \quad (\text{A7a})$$

$$\partial_{t_1} (\rho \mathbf{u}) + \nabla_1 \cdot (\rho \mathbf{u} \mathbf{u} + p \mathbf{I}) = \rho \mathbf{a}_1, \quad (\text{A7b})$$

$$\partial_{t_1}(\rho E) + \nabla_1 \cdot [(p + \rho E)\mathbf{u}] = \rho \mathbf{u} \cdot \mathbf{a}_1, \quad (\text{A7c})$$

where $p = \rho RT$ is the pressure. Similarly, the moments of Eqs. (A2b) and (A3b) lead to the thermohydrodynamic equations at the order of ε^2 :

$$\partial_{t_2} \rho = 0, \quad (\text{A8a})$$

$$\partial_{t_2}(\rho \mathbf{u}) + \nabla_1 \cdot \mathbf{\Pi}^{(1)} = 0, \quad (\text{A8b})$$

$$\partial_{t_2}(\rho E) + \nabla_1 \cdot \mathbf{Q}^{(1)} = 0, \quad (\text{A8c})$$

where $\mathbf{\Pi}^{(1)} = \int \xi \xi \xi f^{(1)} d\xi$ and $\mathbf{Q}^{(1)} = \int \xi \xi h^{(1)} d\xi$.

Note that from Eq. (A7) we can obtain that

$$\partial_{t_1} p + \nabla_1 \cdot (p \mathbf{u}) = -\frac{2}{D} p \nabla_1 \cdot \mathbf{u}, \quad (\text{A9a})$$

$$\partial_{t_1}(\rho \mathbf{u} \mathbf{u}) + \nabla_1 \cdot (\rho \mathbf{u} \mathbf{u} \mathbf{u}) = -[\mathbf{u} \nabla p]_s + \rho [\mathbf{a} \mathbf{u}]_s, \quad (\text{A9b})$$

$$\partial_{t_1}(p \mathbf{u}) + \nabla_1 \cdot (p \mathbf{u} \mathbf{u}) = -RT \nabla_1 p + p \mathbf{a}_1 - \frac{2}{D} (\nabla \cdot \mathbf{u}) p \mathbf{u}, \quad (\text{A9c})$$

$$\begin{aligned} \partial_{t_1}(\rho E \mathbf{u}) + \nabla_1 \cdot [(p + \rho E) \mathbf{u} \mathbf{u}] \\ = \rho \mathbf{u} (\mathbf{u} \cdot \mathbf{a}_1) + \rho E \mathbf{a}_1 - E \nabla p + p \mathbf{u} \cdot \nabla \mathbf{u}, \end{aligned} \quad (\text{A9d})$$

where the symbol $[\cdot]_s$ denotes the symmetric summation of the bracketed second-order tensor, such as $[\mathbf{A}]_s = \mathbf{A} + \mathbf{A}^T$ (the superscript T denotes the transpose of the tensor). With the aids of these results and Eqs. (A6c) and (A6d), we can obtain from Eqs. (A2b) and (A3b) that

$$\begin{aligned} -\frac{1}{\tau_f} \mathbf{\Pi}^{(1)} &= \partial_{t_1} \mathbf{\Pi}^{(0)} + \nabla_1 \cdot \int \xi \xi \xi f^{(0)} d\xi + \mathbf{a}_1 \cdot \int \xi \xi \nabla \xi f^{(0)} d\xi \\ &= \partial_{t_1} p \mathbf{I} + \partial_{t_1}(\rho \mathbf{u} \mathbf{u}) + [\nabla_1(p \mathbf{u})]_s + \nabla_1 \cdot (p \mathbf{u}) \mathbf{I} \\ &\quad + \nabla_1 \cdot (\rho \mathbf{u} \mathbf{u} \mathbf{u}) - \rho [\mathbf{a}_1 \mathbf{u}]_s = p \left(\mathbf{S}_1 - \frac{2}{D} (\nabla_1 \cdot \mathbf{u}) \mathbf{I} \right) \end{aligned} \quad (\text{A10})$$

and

$$\begin{aligned} -\frac{1}{\tau_h} \mathbf{Q}^{(1)} + \frac{1}{\tau_{hf}} \mathbf{\Pi}^{(1)} \cdot \mathbf{u} + \mathbf{\Pi}^{(0)} \cdot \mathbf{a} \\ = \partial_{t_1} \mathbf{Q}^{(0)} + \nabla_1 \cdot \int \xi \xi \xi h^{(0)} d\xi + \mathbf{a}_1 \cdot \int \xi \xi \nabla \xi h^{(0)} d\xi \\ = \partial_{t_1}(p \mathbf{u}) + \partial_{t_1}(\rho E \mathbf{u}) + \nabla_1 [p(RT + E)] \\ \quad + \nabla_1 \cdot (p \mathbf{u} \mathbf{u}) + \nabla_1 \cdot [(p + \rho E) \mathbf{u} \mathbf{u}] - \rho E \mathbf{a}_1 \\ = \mathbf{\Pi}^{(0)} \cdot \mathbf{a}_1 + p \left(R \nabla_1 T - \frac{2}{D} \mathbf{u} (\nabla_1 \cdot \mathbf{u}) + \mathbf{u} \cdot \nabla_1 \mathbf{u} + \nabla_1 E \right) \\ = \mathbf{\Pi}^{(0)} \cdot \mathbf{a}_1 + \frac{D+2}{2} p R \nabla_1 T + p \mathbf{u} \cdot \left(\mathbf{S}_1 - \frac{2}{D} (\nabla_1 \cdot \mathbf{u}) \mathbf{I} \right) \end{aligned}$$

$$= \mathbf{\Pi}^{(0)} \cdot \mathbf{a}_1 + \frac{D+2}{2} p R \nabla_1 T - \frac{1}{\tau_f} \mathbf{\Pi}^{(1)} \cdot \mathbf{u},$$

or

$$\mathbf{Q}^{(1)} = -\frac{D+2}{2} \tau_h p R \nabla_1 T + \mathbf{\Pi}^{(1)} \cdot \mathbf{u}, \quad (\text{A11})$$

where $\mathbf{S}_1 = [\nabla_1 \mathbf{u}]_s$.

Combining the first- and the second-order results (A7) and (A8), together with Eqs. (A10) and (A11), we arrived at the thermohydrodynamic equations at the Navier-Stokes order,

$$\partial_t \rho + \nabla \cdot (\rho \mathbf{u}) = 0, \quad (\text{A12a})$$

$$\partial_t(\rho \mathbf{u}) + \nabla \cdot (\rho \mathbf{u} \mathbf{u}) = -\nabla p + \nabla \cdot \boldsymbol{\tau} + \rho \mathbf{a}, \quad (\text{A12b})$$

$$\partial_t(\rho E) + \nabla \cdot [(p + \rho E)\mathbf{u}] = \nabla \cdot (\lambda \nabla T) + \nabla \cdot (\boldsymbol{\tau} \cdot \mathbf{u}) + \rho \mathbf{u} \cdot \mathbf{a}, \quad (\text{A12c})$$

where $\boldsymbol{\tau} = \mu [\mathbf{S} - (2/D)(\nabla \cdot \mathbf{u}) \mathbf{I}]$, and

$$\mu = \tau_f p \quad \text{and} \quad \lambda = \frac{(D+2)R}{2} \tau_h p$$

are the viscosity and thermal conductivity, respectively.

APPENDIX B: THE HYDRODYNAMIC EQUATIONS OF THE DISCRETE VELOCITY MODEL

The Chapman-Enskog analysis of the DVM (42) is similar to that presented in Appendix A. The main differences lies in the terms relevant to the temperature. Specifically, with the following Chapman-Enskog expansions,

$$\partial_t = \sum_{n=1}^{\infty} \varepsilon^n \partial_{t_n}, \quad \nabla = \varepsilon \nabla_1, \quad \mathbf{a} = \varepsilon \mathbf{a}_1, \quad (\text{B1a})$$

$$f_i = \sum_{n=0}^{\infty} \varepsilon^n f_i^{(n)}, \quad h_i = \sum_{n=0}^{\infty} \varepsilon^n h_i^{(n)}, \quad (\text{B1b})$$

we have

$$F_i = \varepsilon F_i^{(1)}, \quad q_i = \varepsilon q_i^{(1)} + \varepsilon^2 q_i^{(2)} + \dots,$$

with

$$F_i^{(1)} = w_i \rho \left(\frac{\mathbf{c}_i \cdot \mathbf{a}_1}{RT_0} + \frac{(\mathbf{c}_i \cdot \mathbf{a}_1)(\mathbf{c}_i \cdot \mathbf{u})}{(RT_0)^2} - \frac{\mathbf{a}_1 \cdot \mathbf{u}}{RT_0} \right),$$

$$q_i^{(1)} = w_i \rho E (\mathbf{c}_i \cdot \mathbf{a}_1) / RT_0 + f_i^{(0)} \mathbf{c}_i \cdot \mathbf{a}_1,$$

$$q_i^{(k)} = f_i^{(k-1)} \mathbf{c}_i \cdot \mathbf{a}_1 \quad \text{for } k > 1.$$

Furthermore, it can be easily verified that

$$\sum_i f_i^{(n)} = 0, \quad \sum_i \mathbf{c}_i f_i^{(n)} = \mathbf{0}, \quad \sum_i h_i^{(n)} = 0 \quad (\text{B2})$$

for $n > 0$, and

$$\Pi_{\alpha\beta}^{(0)} = \sum_i c_{i\alpha} c_{i\beta} f_i^{(0)} = p_0 \delta_{\alpha\beta} + \rho u_\alpha u_\beta, \quad (\text{B3a})$$

$$Q_\alpha^{(0)} = \sum_i c_{i\alpha} h_i^{(0)} = (p_0 + \rho E) u_\alpha, \quad (\text{B3b})$$

$$\sum_i c_{i\alpha} c_{i\beta} c_{i\gamma} f_i^{(0)} = p_0 (u_\alpha \delta_{\beta\gamma} + u_\beta \delta_{\alpha\gamma} + u_\gamma \delta_{\alpha\beta}), \quad (\text{B3c})$$

$$\sum_i c_{i\alpha} c_{i\beta} h_i^{(0)} = p_0 (RT_0 + E) \delta_{\alpha\beta} + (2p_0 + \rho E) u_\alpha u_\beta, \quad (\text{B3d})$$

where $f_i^{(0)} = f_i^{(eq)}$ and $h_i^{(0)} = h_i^{(eq)}$. It is also noted that

$$\sum_i F_i = 0, \quad \sum_i \mathbf{c}_i F_i = \rho \mathbf{a}, \quad \sum_i \mathbf{c}_i \mathbf{c}_i F_i = \rho [\mathbf{a} \mathbf{u}]_s, \quad (\text{B4a})$$

$$\sum_i q_i = \rho \mathbf{u} \cdot \mathbf{a}, \quad \sum_i \mathbf{c}_i q_i = (\rho E \mathbf{I} + \mathbf{\Pi}) \cdot \mathbf{a}. \quad (\text{B4b})$$

where $\mathbf{\Pi} = \sum_i \mathbf{c}_i \mathbf{c}_i f_i$. Therefore, the first-order equations in the expansion of the discrete kinetic equations (42),

$$D_{it_1} f_i^{(0)} = -\frac{f_i^{(1)}}{\tau_f} + F_i^{(1)}, \quad (\text{B5a})$$

$$D_{it_1} h_i^{(0)} = -\frac{h_i^{(1)}}{\tau_h} + \frac{Z_i f_i^{(1)}}{\tau_{hf}} + q_i^{(1)}, \quad (\text{B5b})$$

where $D_{it_1} = \partial_{t_1} + \mathbf{c}_i \cdot \nabla_1$ can lead to the following first-order thermohydrodynamic equations:

$$\partial_{t_1} \rho + \nabla_1 \cdot (\rho \mathbf{u}) = 0, \quad (\text{B6a})$$

$$\partial_{t_1} (\rho \mathbf{u}) + \nabla_1 \cdot (\rho \mathbf{u} \mathbf{u} + p_0 \mathbf{I}) = \rho \mathbf{a}_1, \quad (\text{B6b})$$

$$\partial_{t_1} (\rho E) + \nabla_1 \cdot [(p_0 + \rho E) \mathbf{u}] = \rho \mathbf{u} \cdot \mathbf{a}_1. \quad (\text{B6c})$$

With these results, we can further obtain that $\mathbf{\Pi}^{(1)} \equiv \sum_i \mathbf{c}_i \mathbf{c}_i f_i^{(1)}$ and $\mathbf{Q}^{(1)} \equiv \sum_i \mathbf{c}_i h_i^{(1)}$ have the following expressions:

$$\begin{aligned} -\frac{1}{\tau_f} \mathbf{\Pi}^{(1)} &= \partial_{t_1} \mathbf{\Pi}^{(0)} + \nabla_1 \cdot \sum_i \mathbf{c}_i \mathbf{c}_i f_i^{(0)} - \rho [\mathbf{a}_1 \mathbf{u}]_s \\ &= \partial_{t_1} p_0 \mathbf{I} + \partial_{t_1} (\rho \mathbf{u} \mathbf{u}) + [\nabla_1 (p_0 \mathbf{u})]_s \\ &\quad + \nabla_1 \cdot (p_0 \mathbf{u}) \mathbf{I} - \rho [\mathbf{a}_1 \mathbf{u}]_s \\ &= p_0 \mathbf{S}_1 \end{aligned} \quad (\text{B7})$$

and

$$\begin{aligned} -\frac{1}{\tau_h} Q_\alpha^{(1)} &= \partial_{t_1} Q_\alpha^{(0)} + \partial_{1\beta} \sum_i c_{i\alpha} c_{i\beta} h_i^{(0)} - \frac{1}{\tau_{hf}} \Pi_{\alpha\beta}^{(1)} u_\beta - \sum_i c_{i\alpha} q_i^{(1)} \\ &= \partial_{t_1} [(p_0 + \rho E) u_\alpha] + \partial_{1\beta} [p_0 (RT_0 + E) \delta_{\alpha\beta} + (2p_0 + \rho E) u_\alpha u_\beta] - \frac{1}{\tau_{hf}} \Pi_{\alpha\beta}^{(1)} u_\beta - [(p_0 + \rho E) a_\alpha + \rho (\mathbf{u} \cdot \mathbf{a}_1) u_\alpha] \\ &= [\partial_{t_1} (p_0 u_\alpha) + \partial_{1\beta} (p_0 RT_0 \delta_{\alpha\beta} + p_0 u_\alpha u_\beta)] + \{\partial_{t_1} (\rho E u_\alpha) + \partial_{1\beta} [p_0 E \delta_{\alpha\beta} + (p_0 + \rho E) u_\alpha u_\beta]\} \\ &\quad + \frac{\tau_f}{\tau_{hf}} p_0 S_{\alpha\beta}^{(1)} u_\beta - [(p_0 + \rho E) a_\alpha + \rho (\mathbf{u} \cdot \mathbf{a}_1) u_\alpha] \\ &= RT_0 [\partial_{t_1} (\rho u_\alpha) + \partial_{1\alpha} p_0 + \partial_{1\beta} (\rho u_\alpha u_\beta)] + u_\alpha \{\partial_{t_1} (\rho E) + \partial_{1\beta} [(p_0 + \rho E) u_\beta]\} + \rho E [\partial_{t_1} (u_\alpha) + u_\beta \partial_{1\beta} u_\alpha] \\ &\quad + p_0 u_\beta \partial_{1\beta} u_\alpha + \partial_{1\alpha} (p_0 E) + \frac{\tau_f}{\tau_{hf}} p_0 S_{\alpha\beta}^{(1)} u_\beta - [(p_0 + \rho E) a_\alpha + \rho (\mathbf{u} \cdot \mathbf{a}_1) u_\alpha] \\ &= p_0 a_\alpha + \rho (\mathbf{u} \cdot \mathbf{a}_1) u_\alpha + E (\rho a_\alpha - \partial_{1\alpha} p_0) + p_0 u_\beta \partial_{1\beta} u_\alpha + p_0 \partial_{1\alpha} E + E \partial_{1\alpha} p_0 + \frac{\tau_f}{\tau_{hf}} p_0 S_{\alpha\beta}^{(1)} u_\beta - [(p_0 + \rho E) a_\alpha + \rho (\mathbf{u} \cdot \mathbf{a}_1) u_\alpha] \\ &= p_0 (u_\beta \partial_{1\beta} u_\alpha + \partial_{1\alpha} E) + \frac{\tau_f}{u_{hf}} S_{\alpha\beta}^{(1)} u_\beta = p_0 c_v \partial_{1\alpha} T + p_0 S_{\alpha\beta}^{(1)} u_\beta + \frac{\tau_f}{\tau_{hf}} p_0 S_{\alpha\beta}^{(1)} u_\beta = p_0 c_v \partial_{1\alpha} T + \frac{\tau_f}{\tau_h} p_0 S_{\alpha\beta}^{(1)} u_\beta, \end{aligned} \quad (\text{B8})$$

where we have neglected the terms of order $(\text{Ma})^3$ in the above deductions. Therefore, from the second-order equations of the DVM,

$$\partial_{t_2} f_i^{(0)} + D_{it_1} f_i^{(1)} = -\frac{f_i^{(2)}}{\tau_f}, \quad (\text{B9a})$$

$$\partial_{t_2} h_i^{(0)} + D_{it_1} h_i^{(1)} = -\frac{h_i^{(2)}}{\tau_h} + \frac{Z_i f_i^{(2)}}{\tau_{hf}} + q_i^{(2)}, \quad (\text{B9b})$$

we can easily obtain the thermohydrodynamic equations at the second order of ε^2 :

$$\partial_{t_2}\rho = 0, \quad (\text{B10a})$$

$$\partial_{t_2}(\rho\mathbf{u}) + \nabla_1 \cdot \mathbf{\Pi}^{(1)} = 0, \quad (\text{B10b})$$

$$\partial_{t_2}(\rho E) + \nabla_1 \cdot \mathbf{Q}^{(1)} = 0. \quad (\text{B10c})$$

Finally, based on the results at the orders of ε and ε^2 , we obtain the following thermohydrodynamic equations at the Navier-Stokes level:

$$\partial_t\rho + \nabla \cdot (\rho\mathbf{u}) = 0, \quad (\text{B11a})$$

$$\partial_t(\rho\mathbf{u}) + \nabla \cdot (\rho\mathbf{u}\mathbf{u}) = -\nabla p_0 + \nabla \cdot \boldsymbol{\tau} + \rho\mathbf{a}, \quad (\text{B11b})$$

$$\partial_t(\rho E) + \nabla \cdot [(p_0 + \rho E)\mathbf{u}] = \nabla \cdot (\lambda \nabla T) + \nabla \cdot (\boldsymbol{\tau} \cdot \mathbf{u}) + \rho\mathbf{u} \cdot \mathbf{a}, \quad (\text{B11c})$$

where $\boldsymbol{\tau} = \mu\mathbf{S}$ with $\mu = \tau_f p_0$, and $\lambda = c_v \tau_h p_0$ with $c_v = DR/2$.

-
- [1] P. Lallemand and L.-S. Luo, Phys. Rev. E **68**, 036706 (2003).
 [2] S. Succi, *The Lattice Boltzmann Equation for Fluid Dynamics and Beyond* (Oxford University Press, New York, 2001).
 [3] F. J. Alexander, S. Chen, and J. D. Sterling, Phys. Rev. E **47**, R2249 (1993).
 [4] Y. Qian, J. Sci. Comput. **8**, 231 (1993).
 [5] Y. Chen, H. Ohashi, and M. Akiyama, Phys. Rev. E **50**, 2776 (1994).
 [6] H. Chen, C. Teixeira, and K. Molving, Int. J. Mod. Phys. C **8**, 675 (1997); M. Soe, G. Vahala, P. Pavlo, L. Vahala, and H. Chen, Phys. Rev. E **57**, 4227 (1998).
 [7] G. J. M. Eggle and J. A. Somers, Int. J. Heat Fluid Flow **16**, 357 (1995).
 [8] X. Shan, Phys. Rev. E **55**, 2780 (1997).
 [9] X. He, S. Chen, and G. D. Doolen, J. Comput. Phys. **146**, 282 (1998).
 [10] B. J. Palmer and D. R. Rector, J. Comput. Phys. **161**, 1 (2000).
 [11] Z. L. Guo, B. Shi, and C. Zheng, Int. J. Numer. Methods Fluids **39**, 325 (2002).
 [12] Y. Peng, C. Shu, and Y. T. Chew, Phys. Rev. E **68**, 026701 (2003).
 [13] Y. Shi, T. S. Zhao, and Z. L. Guo, Phys. Rev. E **70**, 066310 (2004).
 [14] G. Barrios, R. Rechtman, J. Rojas, and R. Tovar, J. Fluid Mech. **522**, 9 (2005).
 [15] T. Watanabe, Phys. Lett. A **321**, 185 (2004).
 [16] T. Watanabe, Phys. Fluids **16**, 972 (2004).
 [17] A. D'Orazio and S. Succi, FGCS, Future Gener. Comput. Syst. **20**, 935 (2004).
 [18] A. D'Orazio, M. Corcione, and G. P. Celata, Int. J. Therm. Sci. **43**, 575 (2004).
 [19] C. Shu, X. Niu, and Y. T. Chew, J. Stat. Phys. **121**, 239 (2005).
 [20] C.-H. Wang and R. Yang, Appl. Math. Comput. **173**, 1246 (2006).
 [21] Y. Shi, T. S. Zhao, and Z. L. Guo, Comput. Fluids **35**, 1 (2006).
 [22] H. N. Dixit and V. Babu, Int. J. Heat Mass Transfer **49**, 727 (2006).
 [23] D. Chatterjee and S. Chakraborty, Phys. Lett. A **351**, 359 (2006).
 [24] S. Chapman and T. G. Cowling, *The Mathematical Theory of Non-Uniform Gases*, 3rd ed. (Cambridge University Press, Cambridge, U.K., 1970).
 [25] P. L. Bhatnagar, E. P. Gross, and M. Krook, Phys. Rev. **94**, 511 (1954).
 [26] L. H. Holway, Phys. Fluids **9**, 1658 (1966).
 [27] C. Cercignani, *The Boltzmann Equation and Its Applications* (Springer, Berlin, 1988).
 [28] L. C. Woods, *An Introduction to the Kinetic Theory of Gases and Magnetoplasmas* (Oxford University Press, Oxford, 1993).
 [29] K. H. Prendergast and K. Xu, J. Comput. Phys. **107**, 53 (1993).
 [30] T. Abe, J. Comput. Phys. **131**, 241 (1997).
 [31] X. He and L.-S. Luo, Phys. Rev. E **55**, R6333 (1997); **56**, 6811 (1997).
 [32] X. Shan and X. He, Phys. Rev. Lett. **80**, 65 (1998); X. Shan, X.-F. Yuan, and H. Chen, J. Fluid Mech. **550**, 413 (2006).
 [33] Y. H. Qian, D. d'Humieres, and P. Lallemand, Europhys. Lett. **17**, 479 (1992).
 [34] Z. Guo, C. Zheng, and B. Shi, Phys. Rev. E **65**, 046308 (2002).
 [35] Z. L. Guo, C. Zheng, and B. Shi, Chin. Phys. **11**, 0366 (2002).
 [36] Z. L. Guo, C. Zheng, and B. Shi, Phys. Fluids **14**, 2007 (2002).
 [37] G. H. Tang, W. Q. Tao, and Y. L. He, Phys. Rev. E **72**, 016703 (2005).
 [38] V. A. F. Costa, Int. J. Numer. Methods Fluids **48**, 2333 (2005).
 [39] M. Hortmann M and M. Perić, Int. J. Numer. Methods Fluids **11**, 189 (1990).
 [40] G. Barakos, E. Mitsoulis, and D. Assimacopoulos, Int. J. Numer. Methods Fluids **18**, 695 (1994).